Exploring Biomolecular Self-Assembly with Far-Infrared Radiation

Subjects: Biophysics

Contributor: Takayasu Kawasaki , Yuusuke Yamaguchi , Hideaki Kitahara , Akinori Irizawa , Masahiko Tani

Physical engineering technology using far-infrared radiation has been gathering attention in chemical, biological, and material research fields. In particular, the high-power radiation at the terahertz region can give remarkable effects on biological materials distinct from a simple thermal treatment. Self-assembly of biological molecules such as amyloid proteins and cellulose fiber plays various roles in medical and biomaterials fields. A common characteristic of those biomolecular aggregates is a sheet-like fibrous structure that is rigid and insoluble in water, and it is often hard to manipulate the stacking conformation without heating, organic solvents, or chemical reagents.

terahertz far-infrared radiation amyloid cellulose

1. Introduction

In these days, far-infrared radiation has been frequently employed in chemical and biomedical research fields. For example, microwave heating can be applicable for solid-phase peptide synthesis and metal-based nanoparticle preparations [1][2]. In addition, far-infrared lasers are often employed for biomedical research using cancer cell lines to develop phototherapies and photo-diagnostics [3][4][5]. The high permeability to the biological tissue is also effective for in vivo bioimaging [6]. Nonetheless, the target substances are often heated by the radiation, and while the far-infrared radiation can cause remarkable structural changes of target biomolecules, whether the radiation effect is thermal or non-thermal remains unclear. The wavelengths in the terahertz region usually range from 30 to 3000 μm and are applied to various studies such as spectroscopy [7], radiation [8], and spectral imaging [9]. Researchers focused on a free-electron laser (FEL) and a submillimeter wave from a gyrotron and recently discovered that the high-power far-infrared radiation can regulate self-association of proteins at different far-infrared wavelengths [10][11][12]. The terahertz FEL (so called THz-FEL) has a double pulse structure that is composed of micro- and macro-pulses, in which the duration of the former is 10–20 ps and that of the latter is 4 μs [13]. The oscillation wavelength covers from 30 to 300 μm, and the irradiation power is given as avg. 5 mJ per macropulse (see for the oscillation system). The submillimeter wave from the gyrotron is a single pulse of 1–2 ms half width having 10 W power [14]. The gyrotron oscillation system nowadays acts as a strong radiation source for nuclear magnetic resonance (NMR) spectroscopy with the dynamic nuclear polarization (DNP) technique [15][16][17]. In addition, hyperthermia treatment using far-infrared radiation is expected to be a candidate for the therapeutic management of cancer [18][19].

2. Promotion of Amyloid Fibrillation by the Submillimeter Wave from Gyrotron

Next, an effect of the submillimeter wave on the protein fibril is shown. The submillimeter wave was tuned to 720 μm and oscillated by a 420 GHz gyrotron. Prior to the irradiation experiments, researchers confirmed that the transmittance of the submillimeter wave against the Eppendorf tube was more than 80% at the 0–2.0 THz region. The temperature increase on the surface of the sample in the tube was only around 5 K compared to the non-irradiation area during the irradiation (**Figure 1**a). In the mid-infrared spectra (**Figure 1**b), the peak intensity at around 1620 cm^{-1} was apparently increased after the irradiation (red) compared to that of before irradiation (black), and the conformational analysis (**Figure 1**c) indicated that β-sheet was increased and α-helix was decreased after the irradiation. Congo red staining (**Figure 1**d, upper) showed that fibrils were apparently increased and SEM observation (bottom) revealed that the fibril structure changed into solid aggregates by the submillimeter wave. The result by X-ray scattering analysis is shown in **Figure 1**e. The inclination of the scattering curve from 3 nm^{-1} to 9 nm^{-1} was larger after the irradiation (red) than that before irradiation (black), which means that the shape of the aggregate was changed into the thick lamellar type [20]. A scattering peak at around 3.8 nm^{-1} corresponds to 1.65 nm of the fibril layer, and this value is quite larger compared to the typical size (0.9–1.0 nm) of amyloid fibril [21]. In addition, a tiny peak at 10.6 nm^{-1} indicates that the protein forms a cross-β-sheet conformation and the interval distance between β-sheet chains is 0.59 nm. This value is slightly larger than the typical size (0.4–0.5 nm) [22].

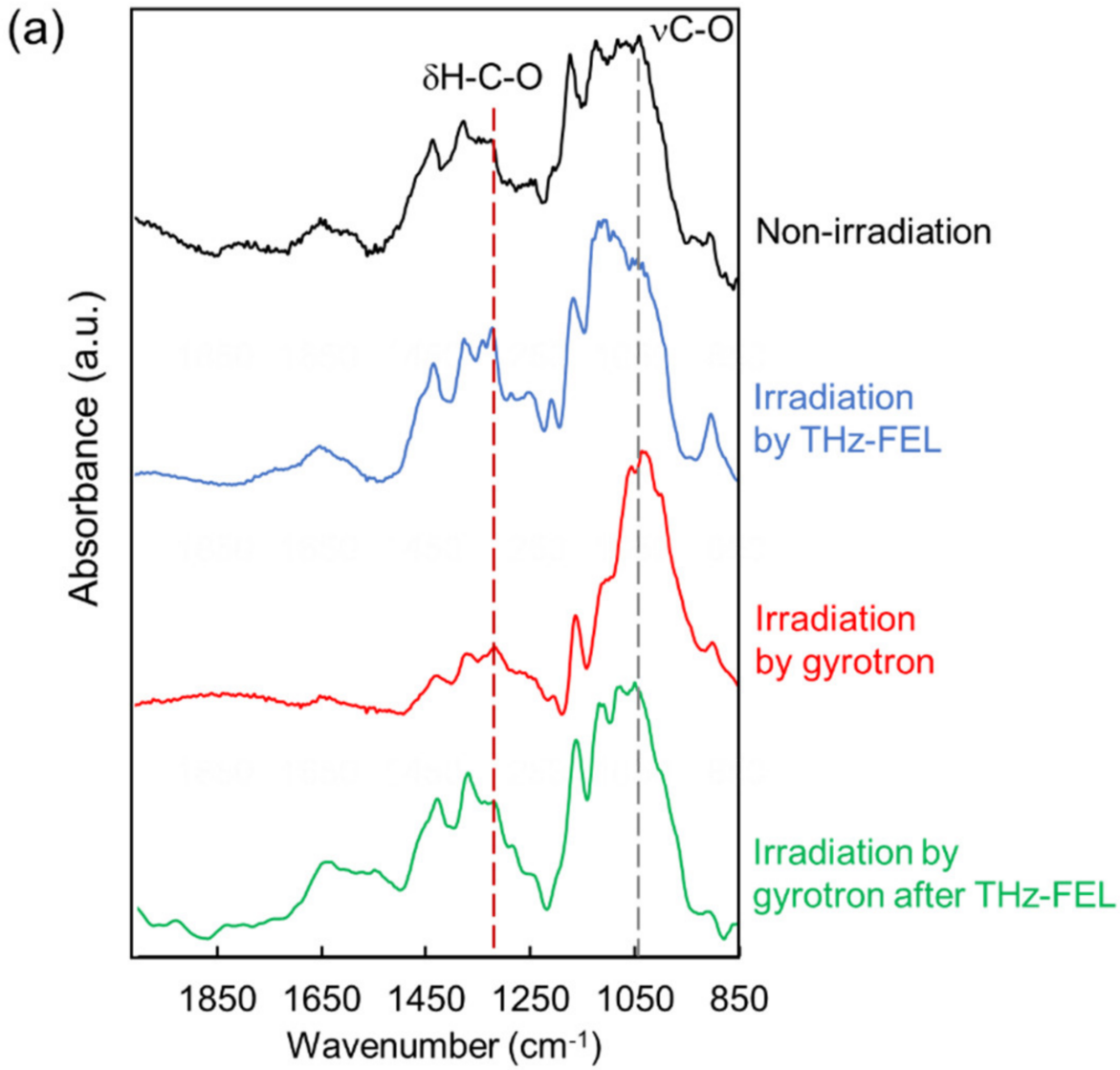
(a)
νC-O
δH-C-O
Non-irradiation
Irradiation
by THz-FEL
Irradiation
by gyrotron
Irradiation by
gyrotron after THz-FEL
Absorbance (a.u.)
1850 1650 1450 1250 1050 850
Wavenumber (cm-1)

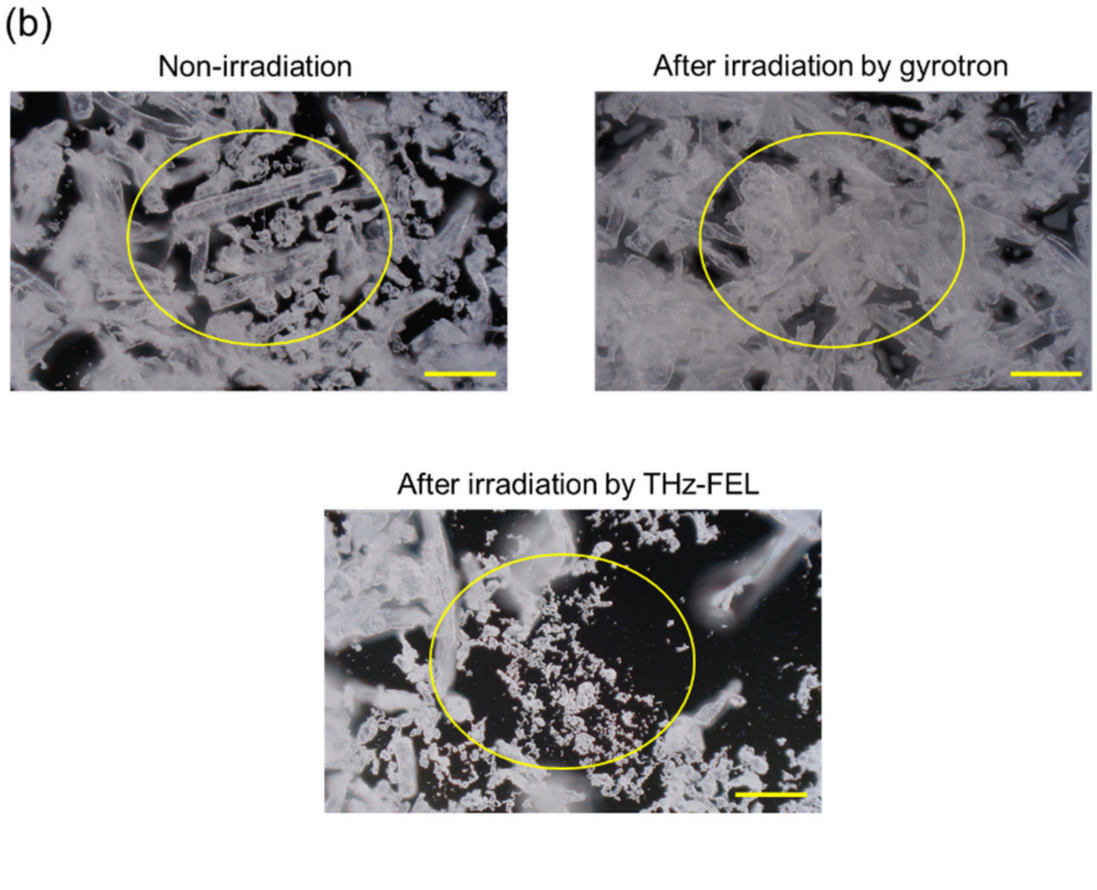
(b)
Non-irradiation
After irradiation by gyrotron
After irradiation by THz-FEL

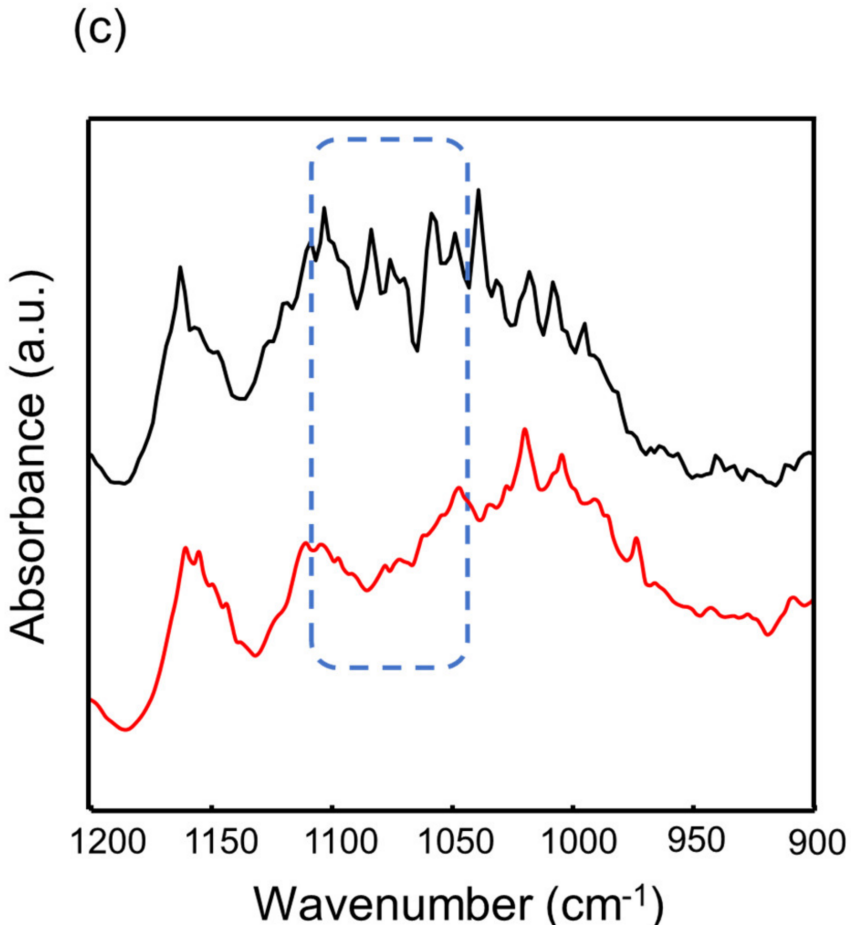
(c)
Absorbance (a.u.)
1200
1150
1100
1050
1000
950
900
Wavenumber (cm-1)

Figure 1. Irradiation Effect of submillimeter wave on lysozyme fibril. (**a**) Thermography camera observation. (**b**) Mid-infrared spectra before (black) and after (red) irradiation. (**c**) Proportions of protein secondary conformations. The color category is the same as (**b**). (**d**) Congo red staining (upper) and SEM observation (bottom) before (−) and after (+) irradiation. White bar: 500 μm; black bar: 1 μm. (**e**) SAXS spectra before (black) and after (red) irradiation: d value equals 2 π q^{-1}.

3. Dissociation and Re-Association of Cellulose Fiber with Far-Infrared Radiation

Researchers explored the applicability of the far-infrared radiation to the other fibrous biomaterials. Cellulose fiber can be developed for cosmetic additives, anti-bacterial sheets, and porous materials in healthcare and pharmaceuticals fields [23][24][25]. In addition, cellulose fibers are applied for components of electronic devices and auto parts in mechanical industries [26][27]. In the mid-infrared spectrum, a strong band at about 1050 cm^{-1} and middle peak around 1300 cm^{-1} were observed (black). The former band corresponds to the stretching vibrational mode of the glycoside bond (νC-O), and the latter peak can be assigned to bending vibration of H-C-O, respectively [28]. When the cellulose was irradiated by the THz-FEL tuned to 80 μm, the former peak was decreased and the latter peak was increased (blue). On the other hand, the former peak was largely increased after irradiation by the submillimeter wave at 720 μm (red). Interestingly, when the cellulose fiber was irradiated by the submillimeter wave after the THz-FEL (green), the whole spectral pattern was almost the same as that of the original cellulose (black). Therefore, it can be considered that the fiber was dissociated to the monomeric form by the THz-FEL, and the monomers were re-aggregated by the submillimeter wave radiation. In the morphological images, solid fibers that are several hundred micrometers in length before irradiation (upper left, yellow circle) were destroyed into a number of small particles after THz-FEL irradiation (below). On the contrary, irradiation by submillimeter wave assembled the fibers more than the original cellulose (upper right). Researchers have ever used a mid-infrared FEL to dissociate the cellulose aggregate for the purpose of obtaining the monomeric sugars for the biorefinery application [29]. The mid-infrared FEL is an accelerator-based intense pulse laser at mid-infrared wavelengths (5–10 μm). The time structure is composed of micro-pulse and macro-pulse, and each duration is 1–2 ps and 2 μs, respectively. The oscillation energy is about 5–10 mJ per a macro-pulse. When the cellulose fiber was irradiated by the mid-infrared FEL at 9.1 μm (νC-O), the absorption bands at 1080–1090 cm^{-1} were largely reduced. This indicates that the glycoside bonds were dissociated and low-molecular weight oligosaccharides were released. On the contrary, the glycoside band around 1080 cm^{-1} survived after the THz-FEL irradiation. Therefore, it can be considered that the cleavage of the glycoside bonds is unlikely and the non-covalent bonds such as hydrogen bonds can be affected in the case of the far-infrared radiation.

4. Future Aspect of the Use of Far-Infrared Radiation in Biological and Material Fields

The above results suggest that the fibrous conformations of biomacromolecules were dissociated by the terahertz laser and associated by the submillimeter wave. This implies that regulation of self-assembly of biomaterials can be performed in one test tube by using far-infrared radiations at different wavelengths. Nonetheless, more consideration regarding the difference in the irradiation effects between the THz-FEL and the submillimeter wave from the gyrotron should be needed because not only wavelength but also time structure is varied. The peak power of a macro-pulse of THz-FEL is quite larger than the case of the gyrotron due to the shorter pulse duration. It can also be estimated that one of factors for regulating the aggregation process of biomolecules is the radiation power. Although the study on this reaction mechanism should be a next subject, the fiber biomaterials can be recycled without any organic solvents or external heating by using both the free-electron lasers and gyrotron continuously, which inspires the use of electromagnetic waves at the terahertz region to a sustainable engineering system of solid textile biomaterials. In addition, it can be expected that several types of structural proteins such as silk fibroin [30][31], keratin fiber [32][33], laminin [34][35], and elastin [36][37] can also be targeted by the far-infrared radiation. Those proteins form highly regularized aggregates, although the molecular sizes are various. It is very interesting how the far-infrared radiation can activate those vibrational states and alter the cell functions related with the biomolecular self-associations.

References

1. Pedersen, S.L.; Tofteng, A.P.; Malik, L.; Jensen, K.J. Microwave heating in solid-phase peptide synthesis. Chem. Soc. Rev. 2011, 41, 1826–1844.
2. Horikoshi, S.; Serpone, N. Microwave Flow Chemistry as a Methodology in Organic Syntheses, Enzymatic Reactions, and Nanoparticle Syntheses. Chem. Rec. 2018, 19, 118–139.
3. Wilmink, G.J.; Rivest, B.D.; Roth, C.C.; Ibey, B.L.; Payne, J.A.; Cundin, L.X.; Grundt, J.E.; Peralta, X.; Mixon, D.G.; Roach, W.P. In vitro investigation of the biological effects associated with human dermal fibroblasts exposed to 2.52 THz radiation. Lasers Surg. Med. 2010, 43, 152–163.
4. Vatansever, F.; Hamblin, M.R. Far infrared radiation (FIR): Its biological effects and medical applications. Photon- Lasers Med. 2012, 1, 255–266.
5. Chiang, I.N.; Pu, Y.S.; Huang, C.Y.; Young, T.H. Far infrared radiation promotes rabbit renal proximal tubule cell proliferation and functional characteristics, and protects against cisplatin-induced nephrotoxicity. PLoS ONE 2017, 12, e0180872.
6. Tewari, P.; Garritano, J.; Bajwa, N.; Sung, S.; Huang, H.; Wang, D.; Grundfest, W.; Ennis, D.B.; Ruan, D.; Brown, E.; et al. Methods for registering and calibrating in vivo terahertz images of cutaneous burn wounds. Biomed. Opt. Express 2018, 10, 322–337.
7. Nibali, V.C.; Havenith, M. New Insights into the Role of Water in Biological Function: Studying Solvated Biomolecules Using Terahertz Absorption Spectroscopy in Conjunction with Molecular Dynamics Simulations. J. Am. Chem. Soc. 2014, 136, 12800–12807.

8. Wilmink, G.J.; Grundt, J.E. Invited Review Article: Current State of Research on Biological Effects of Terahertz Radiation. J. Infrared Millim. Terahertz Waves 2011, 32, 1074–1122.
9. Irizawa, A.; Fujimoto, M.; Kawase, K.; Kato, R.; Fujiwara, H.; Higashiya, A.; Macis, S.; Tomarchio, L.; Lupi, S.; Marcelli, A.; et al. Spatially Resolved Spectral Imaging by A THz-FEL. Condens. Matter 2020, 5, 38.
10. Kawasaki, T.; Tsukiyama, K.; Irizawa, A. Dissolution of a fibrous peptide by terahertz free electron laser. Sci. Rep. 2019, 9, 1–8.
11. Kawasaki, T.; Yamaguchi, Y.; Ueda, T.; Ishikawa, Y.; Yaji, T.; Ohta, T.; Tsukiyama, K.; Idehara, T.; Saiki, M.; Tani, M. Irradi-ation effect of a submillimeter wave from 420 GHz gyrotron on amyloid peptides in vitro. Biomed. Opt. Express 2020, 11, 5341–5351.
12. Kawasaki, T.; Yamaguchi, Y.; Kitahara, H.; Irizawa, A.; Tani, M. Regulation of amyloid fibrils by high-power terahertz radiation. J. Jpn. Soc. Infrared Sci. Technol. 2022, 31, 52–59.
13. Isoyama, G. Development of a Free-Electron Laser in the Terahertz Region. JAS4QoL 2020, 6, 1–10.
14. Idehara, T.; Sabchevski, S.P.; Glyavin, M.; Mitsudo, S. The Gyrotrons as Promising Radiation Sources for THz Sensing and Imaging. Appl. Sci. 2020, 10, 980.
15. Ryan, H.; van Bentum, J.; Maly, T. A ferromagnetic shim insert for NMR magnets – Towards an integrated gyrotron for DNP-NMR spectroscopy. J. Magn. Reson. 2017, 277, 1–7.
16. Nanni, E.A.; Barnes, A.B.; Griffin, R.G.; Temkin, R.J. THz Dynamic Nuclear Polarization NMR. IEEE Trans. Terahertz Sci. Technol. 2011, 1, 145–163.
17. Maly, T.; Debelouchina, G.T.; Bajaj, V.S.; Hu, K.-N.; Joo, C.-G.; Mak–Jurkauskas, M.L.; Sirigiri, J.R.; van der Wel, P.C.A.; Herzfeld, J.; Temkin, R.J.; et al. Dynamic nuclear polarization at high magnetic fields. J. Chem. Phys. 2008, 128, 052211.
18. Mattsson, M.-O.; Simkó, M. Emerging medical applications based on non-ionizing electromagnetic fields from 0 Hz to 10 THz. Med. Devices-Evid. Res. 2019, 12, 347–368.
19. Kok, H.P.; Cressman, E.N.K.; Ceelen, W.; Brace, C.L.; Ivkov, R.; Grüll, H.; ter Haar, G.; Wust, P.; Crezee, J. Heating technology for malignant tumors: A review. Int. J. Hyperthermia. 2020, 37, 711–741.
20. Narayanan, T.; Konovalov, O. Synchrotron Scattering Methods for Nanomaterials and Soft Matter Research. Materials 2020, 13, 752.
21. Squires, A.M.; Devlin, G.L.; Gras, S.L.; Tickler, A.K.; MacPhee, C.E.; Dobson, C.M. X-ray Scattering Study of the Effect of Hydration on the Cross-β Structure of Amyloid Fibrils. J. Am. Chem. Soc. 2006, 128, 11738–11739.

22. Iwata, K.; Fujiwara, T.; Matsuki, Y.; Akutsu, H.; Takahashi, S.; Naiki, H.; Goto, Y. 3D structure of amyloid protofilaments of β2-microglobulin fragment probed by solid-state NMR. Proc. Natl. Acad. Sci. USA 2006, 103, 18119–18124.
23. Bianchet, R.T.; Cubas, A.L.V.; Machado, M.M.; Moecke, E.H.S. Applicability of bacterial cellulose in cosmetics – bibliometric review. Biotechnol. Rep. 2020, 27, e00502.
24. Chien, H.-W.; Tsai, M.-Y.; Kuo, C.-J.; Lin, C.-L. Well-Dispersed Silver Nanoparticles on Cellulose Filter Paper for Bacterial Removal. Nanomaterials 2021, 11, 595.
25. Qin, C.; Yao, M.; Liu, Y.; Yang, Y.; Zong, Y.; Zhao, H. MFC/NFC-Based Foam/Aerogel for Production of Porous Materials: Preparation, Properties and Applications. Materials 2020, 13, 5568.
26. Wang, X.; Yao, C.; Wang, F.; Li, Z. Cellulose-Based Nanomaterials for Energy Applications. Small 2017, 13, 42.
27. Zwawi, M. A Review on Natural Fiber Bio-Composites; Surface Modifications and Applications. Molecules 2021, 26, 404.
28. Mazurek, S.; Mucciolo, A.; Humbel, B.M.; Nawrath, C. Transmission Fourier transform infrared microspectroscopy allows simultaneous assessment of cutin and cell-wall polysaccharides of Arabidopsis petals. Plant J. 2013, 74, 880–891.
29. Kawasaki, T.; Sakai, T.; Zen, H.; Sumitomo, Y.; Nogami, K.; Hayakawa, K.; Yaji, T.; Ohta, T.; Tsukiyama, K.; Hayakawa, Y. Cellulose Degradation by Infrared Free Electron Laser. Energy Fuels 2020, 34, 9064–9068.
30. Rockwood, D.N.; Preda, R.C.; Yücel, T.; Wang, X.; Lovett, M.L.; Kaplan, D.L. Materials fabrication from Bombyx mori silk fibroin. Nat. Protoc. 2011, 6, 1612–1631.
31. Bossi, A.M.; Bucciarelli, A.; Maniglio, D. Molecularly Imprinted Silk Fibroin Nanoparticles. ACS Appl. Mater. Interfaces. 2021, 13, 31431–31439.
32. Wang, L.; Cavaco-Paulo, A.; Xu, B.; Martins, M. Polymeric Hydrogel Coating for Modulating the Shape of Keratin Fiber. Front. Chem. 2019, 7, 749.
33. Gough, C.R.; Callaway, K.; Spencer, E.; Leisy, K.; Jiang, G.; Yang, S.; Hu, X. Biopolymer-Based Filtration Materials. ACS Omega 2021, 6, 11804–11812.
34. Nam, K.; Maruyama, C.L.; Wang, C.-S.; Trump, B.G.; Lei, P.; Andreadis, S.T.; Baker, O.J. Laminin-111-derived peptide conjugated fibrin hydrogel restores salivary gland function. PLoS ONE 2017, 12, e0187069.
35. Besser, R.R.; Bowles, A.C.; Alassaf, A.; Carbonero, D.; Claure, I.; Jones, E.; Reda, J.; Wubker, L.; Batchelor, W.; Ziebarth, N.; et al. Enzymatically crosslinked gelatin–laminin hydrogels for applications in neuromuscular tissue engineering. Biomater. Sci. 2019, 8, 591–606.

36. Schräder, C.U.; Heinz, A.; Majovsky, P.; Karaman Mayack, B.; Brinckmann, J.; Sippl, W.; Schmelzer, C.E.H. Elastin is heterogeneously cross-linked. J. Biol. Chem. 2018, 293, 15107–15119.

37. Roberts, S.; Dzuricky, M.; Chilkoti, A. Elastin-like polypeptides as models of intrinsically disordered proteins. FEBS Lett. 2015, 589, 2477–2486.